Korean J. Chem. Eng., 37(8), 1306-1316 (2020)
DOI: 10.1007/s11814-020-0630-2

pISSN: 0256-1115
eISSN: 1975-7220

INVITED REVIEW PAPER

Effect of carbon nanoscaffolds on hydrogen storage performance of magnesium hydride

Dong Ju Han‡, Ki Ryuk Bang‡, Hyun Cho‡, and Eun Seon Cho†

Department of Chemical and Biomolecular Engineering, Korea Advanced Institute of Science and Technology (KAIST), Daejeon 34141, Korea

(*Received 20 April 2020 • Revised 29 June 2020 • Accepted 7 July 2020*)

Abstract−With a growing concern on climate change, hydrogen has attracted great attention as an alternative energy fuel. The hydrogen economy allows us to accomplish a high level of energy security and realize zero emission. To successfully establish the hydrogen economy, the development of sustainable hydrogen production, storage and fuel cell technologies is important; among them, safe and stable hydrogen storage remains more challenging. In this review, we briefly introduce solid-state hydrogen storage materials, focusing on metal hydrides and hydrogen sorption mechanism with emphasis on the related thermodynamic and kinetic obstacles. To overcome such limits, nanoconfinement is regarded as a representative strategy since it can modify hydrogen sorption kinetics and thermodynamics of metal hydrides. We present a nanoconfinement effect of metal hydrides on hydrogen sorption properties, spotlighting carbon scaffolds for confinement. With a rational design of the composite based on metal hydrides and carbon scaffolds, a potential application of solid-state hydrogen storage will be a stepping-stone on the path to a hydrogen economy.

Keywords: Hydrogen Storage, Metal Hydride, Nanoconfinement, Carbon Materials

INTRODUCTION

Depletion of fossil fuels and irreversible climate changes induced by emissions from fuel combustion have accelerated diversifying renewable energy sources including solar, biomass and hydrogen [1,2]. Among them, hydrogen has been regarded as one of the ultimate carbon-free energy carriers since it does not generate environmentally malicious greenhouse gases, such as carbon dioxide, nitrogen oxides and sulfur oxides upon combustion, along with an advantage that it possesses a high gravimetric energy density compared to other chemical fuels [3]. A comprehensive application of hydrogen energy requires an advancement in key technologies including hydrogen production, storage and distribution. Unfortunately, a successful transition from fossil fuels to hydrogen energy has been retarded, especially due to a lack of efficiency and technical difficulties in storing hydrogen. Particularly, evolution of fuel cell electric vehicle (FCEV) powered by hydrogen expects dramatic progress in on-board hydrogen storage technology [4,5]. For practical use of hydrogen energy in various industries, a safe hydrogen storage technology simultaneously satisfying a high capacity and reversibility is imperative. However, a conventional hydrogen storage method has been relying on compressed gas (up to 700 bar) which has low volumetric storage capacity and intrinsic safety concern due to potential explosion. In the case of liquefied hydrogen, not only does it require tremendous energy to liquefy hydrogen, but some amount of stored hydrogen suffers a loss by evaporation or "boil off" of liquefied hydrogen [6].

For these reasons, solid-state hydrogen storage has attracted constant attention as a safe and efficient storage method, despite its limitation on thermodynamic and kinetic properties associated with de/hydrogenation reaction [7,8]. With respect to solid-state storage systems, the candidate materials can be classified into four groups: 1) metal hydrides, 2) complex hydrides, 3) sorbents, and 4) chemical hydrides. Metal hydrides such as MgH_2 and $LaNi_5H_x$, the most studied hydrogen storage material, can readily release or store hydrogen via a reversible reaction between metallic species and hydrogen molecules, and the hydrogen atoms are stored in nongaseous form with high storage density [9,10]. Complex hydrides such as $LiBH_4$ and $NaAlH_4$ consist of metal cations and hydrogen-containing complex anions where hydrogen atoms are present in a complex form covalently bonded to central atoms such as boron or aluminum. They release hydrogen through multi-step reactions with a formation of multi-phase intermediates, accompanied by poor reversibility [11]. Sorbent materials such as metal-organic framework (MOF) have nano/micro pores and high surface area, which allows hydrogen molecules to be physically adsorbed onto the surface via van der Waals force [7]. Chemical hydrides such as NH_3BH_3 contain covalently bound hydrogen atoms in solid or liquid form with high density of hydrogen; however, the selection of an appropriate catalyst for regeneration is essential because of high reaction enthalpy [12]. Above all, metal hydrides such as magnesium hydride (MgH_2) are one of the most promising materials due to their high storage capacity (theoretical gravimetric and volumetric hydrogen storage capacity of Mg are 7.6 wt% and 110 g L^{-1}, respectively), excellent reversibility and low cost [9,10]. In spite of these benefits, sluggish de/hydrogenation kinetics and thermodynamic stability of metal hydrides require severe pressure and temperature condition for oper-

†To whom correspondence should be addressed.
E-mail: escho@kaist.ac.kr
‡The authors equally contributed to this review.

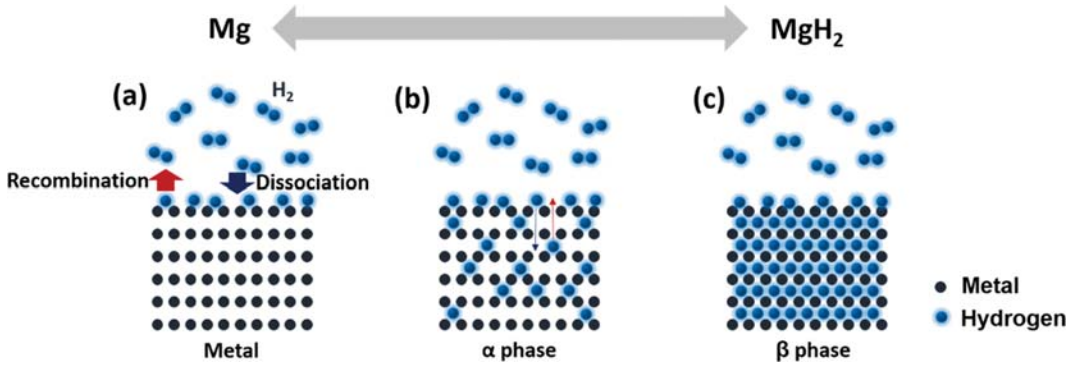

Fig. 1. Illustration of the de/hydrogenation mechanism in metal hydrides: (a) Dissociation of hydrogen molecules or recombination of hydrogen atoms, (b) diffusion of hydrogen atoms into bulk interstitial sites to form an M-H solid solution commonly referred to as α-phase, (c) formation of saturated β-phase of metal hydrides with an increase of hydrogen pressure.

ation, and it still remains as significant challenge to reach technical performance targets for practical hydrogen storage systems [13]. Nevertheless, an outstanding reversibility and high storage capacity makes metal hydrides a good candidate for deploying hydrogen energy. To resolve the aforementioned drawbacks, various strategies have been implemented in terms of material design. It has been widely established that carbon additives and transition metal catalysts enhance the hydrogenation reaction kinetics of metal hydrides, although some portion of storage capacity is sacrificed for the sake of such accelerated kinetics, as a result of considerable dead mass in a total composite [14-16]. On the other hand, nanoscaling contributes to thermodynamic destabilization of metal hydrides, lowering the reaction enthalpy. Also, it is believed that the diffusion path for hydrogen atoms becomes shortened at the nanoscaled metal hydrides, allowing a kinetic improvement [17,18]. Especially, confinement within a nanoscaffold provides additional merits, in which case it prevents agglomeration and oxidation of metal hydrides particles [19,20]. Moreover, it is known that alloying with other elements (rare earth elements, transition metals and partial main group elements) reduces thermodynamic barrier of metal hydrides and changes de/hydrogenation mechanism [21]. Among these strategies, nanoconfinement enables us to generate uniformly dispersed metal hydrides by restricting evolution of particles. In addition to the nanosizing effect, some scaffolds functionalized or doped with hetero-elements show catalytic influences via charge transfer, irrespective of the particle size of metal hydrides.

In this review, we introduce the nanoconfinement of metal hydrides into scaffold materials to advance hydrogen storage properties, particularly focusing on magnesium hydride (MgH_2) as a model system. Hydrogen sorption mechanism of metal hydrides is described to understand the main obstacles to practical application in terms of thermodynamic and kinetic characteristics, and various nanoscaffold materials for the confinement of metal hydrides are presented, laying stress on carbon scaffolds. The improvement of both thermodynamic and kinetic properties for metal hydrides associated with de/hydrogenation is followed as a result of structural manipulation with carbon scaffolds. It also includes the role of such carbon scaffolds in improving hydrogen storage performance of metal hydrides by means of nanoconfinement, simultaneously providing catalytic effects and structural stability.

HYDROGEN SORPTION MECHANISM IN METAL HYDRIDE

The formation of metal hydrides consists of a series of steps involving heterogeneous phase transformation at gas-solid interface where metal (Mg) combines with hydrogen gas (H_2) to produce metal hydride (MgH_2). It can be summarized as the following steps: 1) transport of H_2 onto the surface of Mg, 2) dissociation of H_2 into 2H, 3) chemisorption of H, followed by diffusion from surface to bulk, and 4) nucleation and growth of MgH_2 (Fig. 1). The first step depends on collision of hydrogen molecules onto the Mg surface. Accordingly, a high surface area with abundant active sites is required to ensure a sufficient supply of H_2 [22,23]. The adsorbed H_2 is dissociated into two hydrogen atoms on the surface of Mg. In the subsequent step, the hydrogen atoms form a chemical bond with Mg initiated from the surface, moving into the tetrahedral interstitial sites within the lattice structure, which results

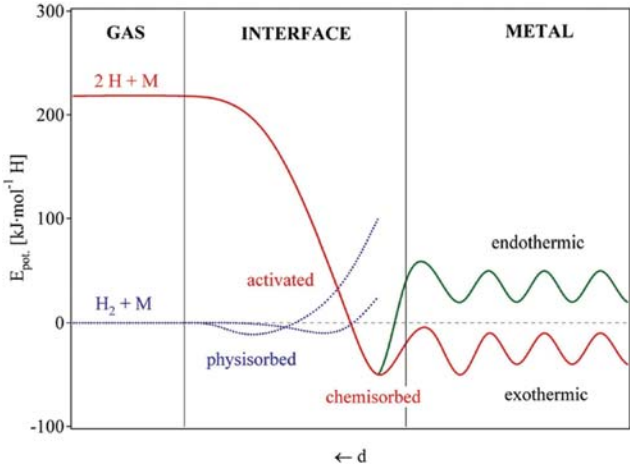

Fig. 2. Simplified one-dimensional energy barrier curve for de/hydrogenation of metal hydrides, showing separated individual energy barriers from each step; in initial reaction, the dissociation of H_2 into the hydrogen atoms on the metal surface is a rate-limiting step due to the high potential energy to split hydrogen molecules into atoms. Reprinted from ref. [26], Copyright 2003, with permission from Elsevier.

in a partial conversion to tetragonal α-phase of MgH_2 at low hydrogen concentration. At more concentrated hydrogen condition, the hydrogen atoms promote the evolution of the β-phase, and the antecedent α-phase is transformed into β-MgH_2 [24]. The decomposition of the metal hydrides into the metal, corresponding to hydrogen desorption, is the reverse of the above-mentioned mechanism. In the case of absorption, the overall energy barrier consists of the separated individual energy barriers from each step, which includes energy for hydrogen adsorption, dissociation, chemisorption, penetration into the subsurface, diffusion in the bulk, and nucleation and growth of hydrides (Fig. 2). In the initial process, it is believed that the dissociation into the hydrogen atoms on the surface is the slowest step owing to the high energy to split the hydrogen molecules [25,26]. On this basis, incorporation of various catalysts (e.g., Pd, Ni, Ti) into metal hydrides has been considered to reduce the energy barrier for dissociation of hydrogen molecules and diffusion away from the catalytic site. However, as hydrogenation progresses, the diffusion of hydrogen atoms through the β-MgH_2 phase also can be regarded as the rate-limiting step, prior to the nucleation and growth of the hydride phase [22,27,28]. On the other hand, defects or grain boundaries present in the metal hydride can affect their overall reaction rate by providing quick pathways for transportation of hydrogen atoms [23,29,30]. Thus, the de/hydrogenation kinetics and related rate limiting steps depend on structural variables, which can be modulated via synthetic methods or by forming a composite with other scaffold materials. To comprehensively understand the rate limiting steps, several kinetic models have been studied, including Jander and Johnson-Mehl-Abrami-Kolmogorov (JMAK) models with the assumptions that the hydride has similar size, shape, surface reactivity and defects (Fig. 3) [31,32]. However, none of such models have been conclusively proven to be employed generally since de/hydrogenation reaction involves the multi-steps of the hydride decomposition/formation. Therefore, the explanation for rate limiting step via a specific model should be subordinate to the accuracy of fitting.

With regard to thermodynamics, Gibbs energy change is the key driving force for the de/hydrogenation reaction; thus, the metal hydride system including Mg has been modified to induce the

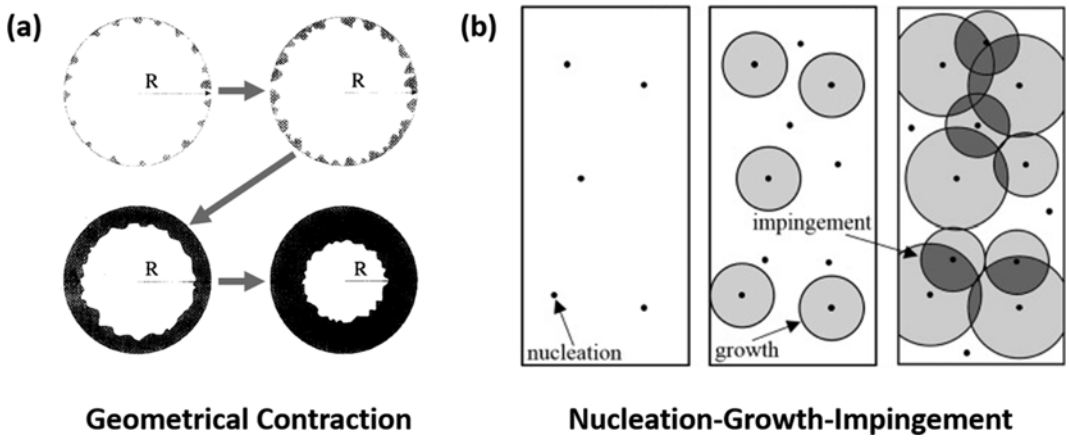

Fig. 3. Representative rate limiting step models: (a) Geometrical contraction models including contracting volume, Jander, Ginstling-Broundshtein (G-B) and Valensi-Carter (V-C). Reprinted from ref. [32], Copyright 1995, with permission from Elsevier, (b) nucleation-growth-impingement models which are generally regarded as Jonhson-Mehl-Avrami-Kolomogorov (JMAK) models. Reprinted from ref. [31], Copyright 2016, with permission from Elsevier.

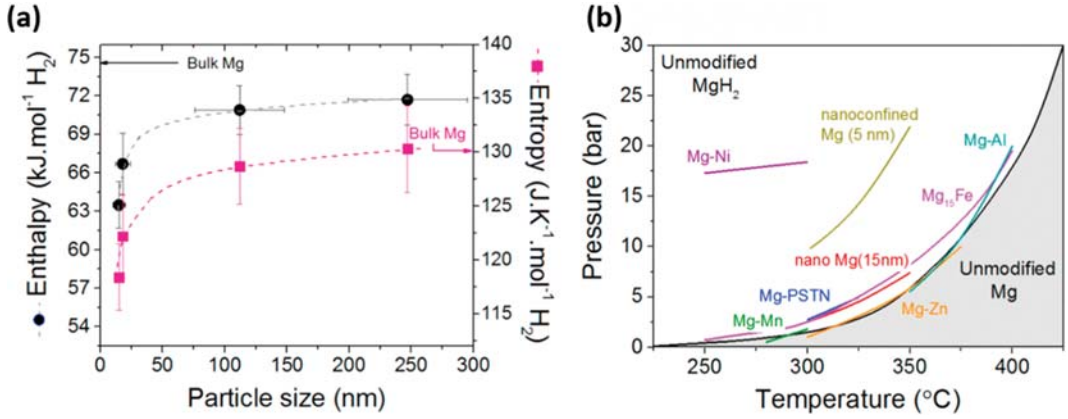

Fig. 4. General methods for controlling thermodynamic property of metal hydrides: (a) Enthalpy and entropy change as function of particle size of Mg, (b) temperature dependence of the dissociation pressure of MgH_2 for various modified types. Reprinted from ref. [16], Copyright 2018, with permission from Elsevier.

change of thermodynamic parameters, modulating an interplay between enthalpy and entropy (Fig. 4). A representative approach is to reduce the particle size which exposes more atoms at the surface, resulting in increased surface energy [22,23,27]. The enthalpy for de/hydrogenation can decrease resulting from the excess surface energy in the reduced particle size of Mg by nanoconfinement or electrostatic/steric repulsion with surfactants [33-35]. In addition, the formation of metastable phases (γ-MgH_2) with different crystalline structure and stability compared to the β-MgH_2 phase facilitates hydrogen diffusion and H atomic motion, attributed to the lower migration barrier [36-39]. Also, it has been proposed that the addition of a compressive stress to Mg by structural modification provides destabilization of the Mg-H bond induced by the elastic constraint, while it also leads to a repulsive interaction between hydrogen atoms in metal lattice structure [40,41].

SCAFFOLD MATERIALS FOR COMPOSITE WITH METAL HYDRIDES

For an improvement in thermodynamic and kinetic properties of metal hydrides associated with de/hydrogenation, numerous studies have focused on the nanoconfinement into a variety of scaffold materials, which include polymer [20,42,43], carbon materials [44-46], mesoporous silica scaffolds [44,47] and metal-organic framework (MOF) [48,49] (Fig. 5). These scaffold materials for nanoconfinement typically have a controlled pore size and a high surface area, also with a capability for facile surface modification to introduce further functionalities. In addition, they should be able to maintain structural robustness under de/hydrogenation condition. The pore size of scaffolds can be controlled by the synthetic condition, resulting in different size of metal hydride nanoparticles. Metal hydrides can be incorporated with scaffolds via a solvothermal method [20] or a solvent/melt infiltration [50-52].

Polymer materials such as poly(methyl methacrylate) (PMMA) [20,43] and methacrylate-based block copolymer [42] have been used as a scaffold material for metal and complex hydrides. Jeon et al. reported a synthetic method to fabricate air-stable Mg nanocomposites by using PMMA [20]. PMMA can protect the surface of Mg nanoparticles from water and oxygen due to its hydrogen selective-permeable property, leading to an improvement in cyclability and hydrogen storage performance. In addition, Gosalawit-Utke et al. used a block copolymer, which is the PMMA-co-butyl methacrylate (PMMA-co-BM), to fabricate $LiBH_4$ in nano-scale [42]. The onset dehydrogenation temperature of the nano-confined $LiBH_4$ is decreased, and the reactivity of $LiBH_4$ with oxygen and water is dramatically reduced due to the hydrophobicity of the block copolymer, improving cyclability.

Carbon scaffolds such as ordered mesoporous carbons [17,53,54], graphene derivatives [19,55-59], activated carbons [60-65] and graphite [57,66] are the most extensively studied materials for the nanoconfinement of metal hydrides due to an ease of modification with controllable physicochemical properties. Ordered mesoporous carbons such as CMK-3 have interconnected channels for the diffusion of metal hydrides, which makes them adequate for infiltra-

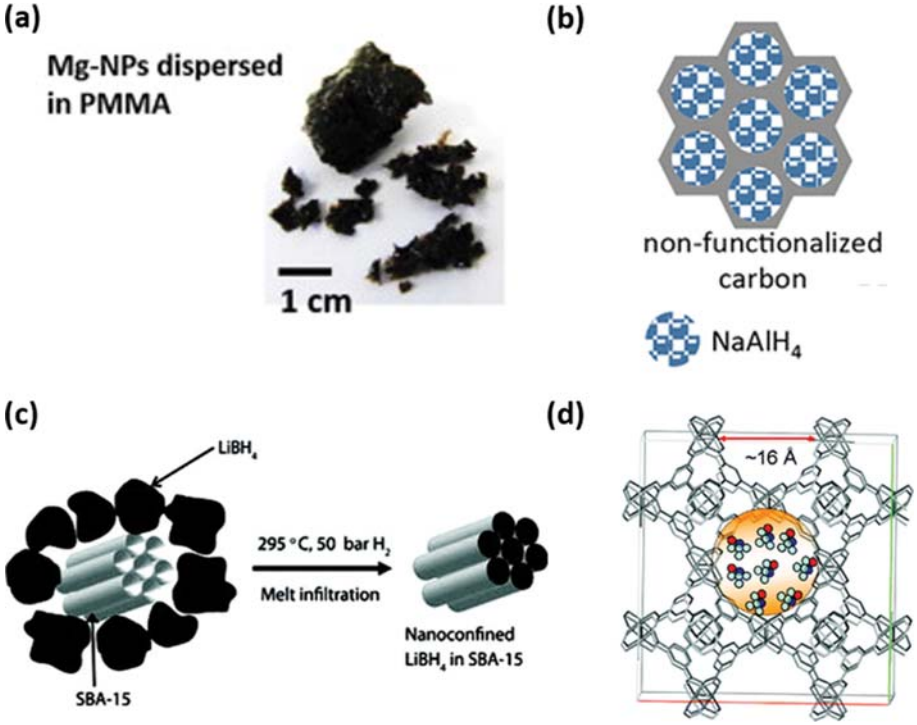

Fig. 5. Schematic illustration of various scaffold/matrix materials with metal hydrides: (a) Polymer. Reprinted from ref. [43], Copyright 2013, with permission from Elsevier, (b) porous carbon scaffold. Reprinted with permission from ref. [46], Copyright 2018 American Chemical Society, (c) mesoporous silica scaffold (SBA-15). Reprinted with permission from ref. [47], Copyright 2010 American Chemical Society, and (d) metal-organic framework (MOF). Reprinted with permission from ref. [48], Copyright 2009 American Chemical Society.

tion, and metal and complex hydrides confined within CMK-3 exhibit an improvement in hydrogen storage performance. Li et al. reported confined $NaAlH_4$ in CMK-3 via melt impregnation methods [67]. The confined $NaAlH_4$ had enhanced kinetics and cycling stability with high capacity retention of >80%. Similar $NaAlH_4$ composite with higher loading capacity of 45 wt% was synthesized by Minella et al. [51]. The nanoconfinement of Mg within CMK-3 has been reported by several groups including He et al. [53] and Jia et al. [54], where Mg in CMK-3 presents an kinetic enhancement for hydrogen storage. Activated carbon is another attractive scaffold with numerous porous sites. Liu et al. reported Mg nanoparticles confined in carbon aerogels (CA) through the wet impregnation method [55]. The Mg-CA composite showed significantly low activation energy (29.4 kJ/mol H_2) for hydrogen sorption. Gosalawit-Utke et al. also synthesized carbon aerogel-based nanoconfined metal hydride composite [65]. $2LiBH_4$-MgH_2-$TiCl_3$ in resorcinol-formaldehyde carbon aerogel scaffold exhibited improved sorption rate and reversibility. Furthermore, a variety of graphene derivatives have been investigated for confinement of metal hydride due to its high specific surface area and unique chemical/physical properties. Graphene derivatives allow a high encapsulation efficiency for metal hydrides, compared to other carbon materials, due to high surface-to-volume ratio. Xia et al. synthesized monodisperse MgH_2 nanoparticle in graphene (MHGH) with 20-75 wt% loading capacities [56]. The MHGH with Ni nanoparticles had outstanding sorption kinetics and maintained its performance for 100 cycles. The derivatives of graphene such as graphene nanoribbon [68] and nanoplate [69] were also synthesized with Mg and showed improved hydrogen storage properties.

Mesoporous silica scaffolds are also considered promising for encapsulating metal hydrides attributed to mesoporous structure and structural rigidity. The most common types of mesoporous silica scaffolds are MCM-41 [70] and SBA-15 [47,71], which have been widely studied as a stable support structure for hydrogen storage materials. For example, nanoconfined MgH_2 in pores of ordered mesoporous silica (SBA-15), which was prepared by infiltration of $MgBu_2$ solution into the pores followed by freeze drying and hydrogenation treatment, was presented for improvement on dehydrogenation properties by Wang et al. [72]. The nanoscaled MgH_2 exhibited significantly decreased desorption temperature compared to that of unconfined by silica scaffold. In addition, Ngene et al. fabricated a system in which $LiBH_4$ is confined into a mesoporous silica scaffold via the melt filtration method for enhancing hydrogen release kinetics [47]. The silica scaffold effectively restricted the formation of intermediates, such as lithium silicates, from $LiBH_4$ and reduced hydrogen release temperature of $LiBH_4$.

With chemical versatility and controllable pore size, MOF is well-known as a hydrogen storage material via a physical adsorption [73,74], while it can be also employed as a scaffold for metal hydride infiltration with a desired porous structure. Zn [75], Cu [48, 76] and Mg-based MOF [76] have been extensively used as a scaffold material for metal and complex hydrides. For example, Lim et al. fabricated Mg nanocrystals in a porous MOF (SNU-90) [75]. This Mg-MOF nanocomposite can store hydrogen in dual approaches

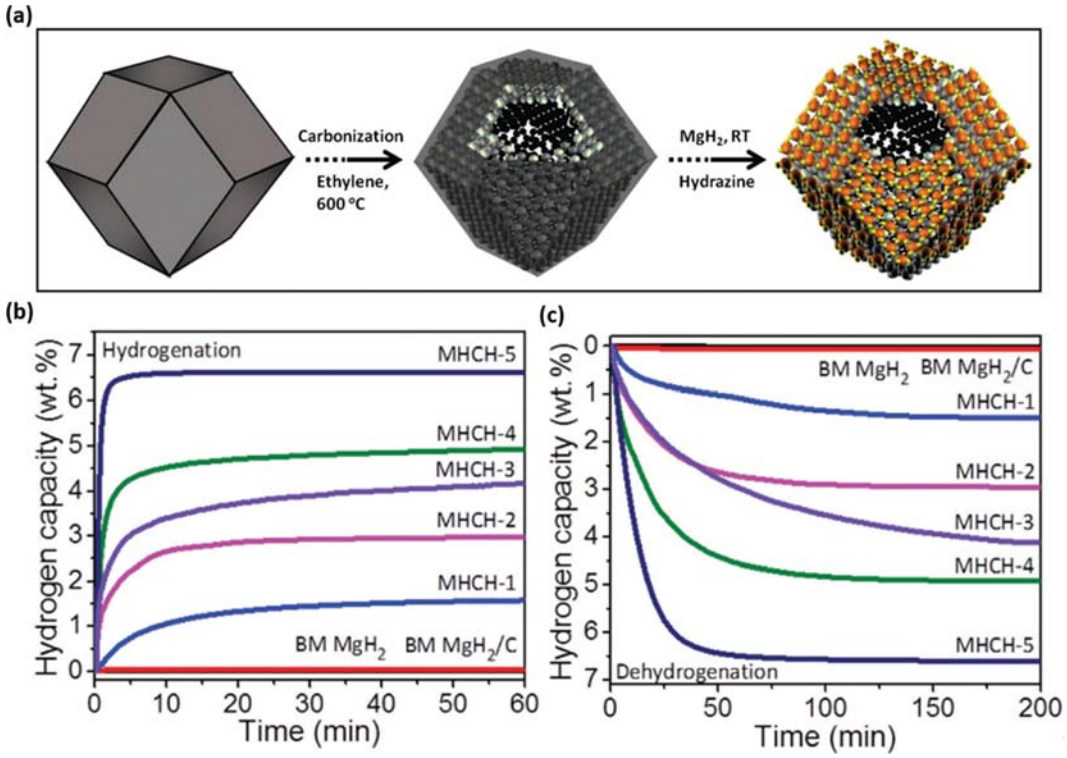

Fig. 6. (a) Schematic representation of the self-assembled MgH_2 nanoparticle on three-dimensional active carbon scaffold. (b) Isothermal hydrogenation and (c) dehydrogenation profiles of the air-stable, nanoconfined, MgH_2 nanoparticle-anchored 3-D carbon architecture (MHCH) samples at 180 °C as compared to ball-milled MgH_2 and MgH_2/C samples. Reprinted with permission from ref. [78], Copyright 2017 Royal Society of Chemistry.

via both the physisorption (MOF-H_2) and chemisorption (nano-sized Mg-H_2). On the other hand, Bhakta et al. reported that $NaAlH_4$ can be confined within the MOF pore, resulting in acceleration of the hydrogen desorption rate [48]. The HKUST-1 was selected as a host MOF to infiltrate $NaAlH_4$ into the pore of MOF, thereby obtaining the confined structure of $NaAlH_4$.

ROLE OF CARBON NANOSCAFFOLDS IN ENHANCING HYDROGEN STORAGE PERFORMANCE OF METAL HYDRIDES

As mentioned, carbon-based materials are a promising and widely used scaffold for the nanoconfinement of metal hydrides with an advantage of physiochemical versatility. A variety of carbon materials such as graphite [66], carbon fiber [61,77] and graphene derivatives [19,21] have been studied as a scaffold of metal and complex hydrides with a facile structural and morphological modification procedure. For example, Shinde et al. developed a MgH_2 nanoparticle embedded into a three-dimensional activated carbon scaffold (Fig. 6) [78]. This scaffold enables MgH_2 to be homogeneously separated in the pore of matrix, suppressing the aggregation of nanoparticles, and the composite exhibited a distinguished hydrogen storage performance with 6.63 wt% of hydrogen storage capacity and rapid hydrogen sorption kinetics at 180 °C. On the other hand, Carr et al. demonstrated the effect of N-doped/undoped nanoporous carbon scaffolds on dehydrogenation properties of the nanoconfined $NaAlH_4$ [46]. They found that the surface chemistry of carbon scaffolds can have a noticeable effect on the activation energy for the desorption process of the confined $NaAlH_4$. The $NaAlH_4$ confined within N-doped carbon scaffold showed a lower activation energy-approximately by 20 kJ/mol-than the one in the undoped counterpart. This result indicates that the hetero-atoms doped over carbon scaffolds lead to the change of the electronic energy level of the metal hydride, resulting in tuning hydrogen sorption kinetics. In addition to ease of surface modification, a high thermal conductivity of carbon materials has a beneficial effect on hydrogen storage performance of the hydrides upon the formation of composites. The effective control of heat transfer during de/hydrogenation reactions of metal or complex hydrides is one of the major challenges to the hydrogen storage system due to a high value of reaction enthalpy, and carbon scaffolds can play a crucial role in thermal management of metal hydrides [7].

Here, we highlight the effects of carbon scaffolds on the hydrogen storage performance of metal hydrides, exploring the related nanoscaling and catalytic effects along with stability of composites. On the basis of understanding structureproperty relationship of the composite, it enables an elaborate material design using carbon scaffolds for an enhancement of hydrogen storage performance of metal hydrides.

1. Effect of Nanoscaling on Hydrogen Storage Properties

Thermodynamic and kinetic properties of metal hydrides associated with hydrogen sorption are dramatically influenced by their size. As mentioned, in the hydrogenation process the adsorbed hydrogen molecule on the surface of the active-metal phase is dissociated into two hydrogen atoms, and these hydrogen atoms are subsequently diffused into the lattice structure to form metal hydride phase. Nanoscaling of metal hydrides can offer opportunities to improve hydrogen storage performance in the following aspects: 1) hydrogen molecules are able to adsorb onto the active-metal surface with a high probability due to high surface-to-volume ratio; 2) the diffusion length of hydrogen atoms from surface to bulk phase is significantly reduced, rapidly forming metal hydride phase; 3) according to theoretical studies, the enthalpy of formation for metal hydrides can decrease via nanostructuring ascribed by surface energy or lattice deformation [79]. In a typical bulk metal and complex hydride, surface energy is inconsequential, whereas the portion of surface energy becomes substantial for a nano-sized counterpart, leading to a reduction in the enthalpy of formation of metal hydrides. In addition, the nanoconfined metal hydrides experience lattice distortion, which induces additional strain fields and structural destabilization, resulting in change of thermodynamic properties for hydrogen sorption.

Nanoscaled metal hydrides can be manipulated by confining within the carbon scaffolds which have a well-defined pored structure to present enhanced hydrogen sorption properties [78]. For example, Zhang et al. developed a new approach to preparing nanoconfined MgH_2 in which $MgBu_2$ precursor is incorporated into carbon aerogel scaffolds, followed by a conversion MgH_2 through the hydrogenation process [80]. In general, it is known that metal hydrides such as MgH_2 are hardly inserted into pore of carbon scaffolds due to their intrinsic rigidity as well as a low solubility in any solvent as opposed to complex hydrides. The nano-confined MgH_2 exhibited five-times faster dehydrogenation rate than ball-milled bulk MgH_2, which is attributed to the high specific surface area of MgH_2, shortened diffusion length of hydrogen atoms, and suppression of aggregation of nanoparticles. Furthermore, Ampoumogli et al. infiltrated complex hydrides, such as $Ca(BH_4)_2$, into CMK-3 scaffold, which has a narrow pore distribution between 3-5 nm [81]. The decomposition temperature of $Ca(BH_4)_2$ with CMK-3 was approximately decreased by 100 °C as compared to bulk $Ca(BH_4)_2$. This result would be caused by destabilization of $Ca(BH_4)_2$ which originates from the mechanical stress under the confined structure and the increased surface to volume ratio of nano-sized $Ca(BH_4)_2$.

2. Stability Improvement via Nanoconfinement

As mentioned, nano-sizing significantly enhances hydrogen storage properties of metal hydrides. The reactive surface of nanoscale metal hydrides certainly promotes the hydrogen sorption reaction, while it also causes an aggregation of nanoparticles during sorption cycles. Accordingly, nanoscale metal hydrides without supporting scaffolds easily lose their structure, nullifying improved performance after several sorption cycles [82-84]. Therefore, preventing structural deformation such as aggregation during de/hydrogenation cycles is essential to maintain the performance of nanoscale metal hydrides. In this respect, confinement in scaffolds provides an adequate route to enhance a structural stability of metal hydrides; particularly, carbon scaffolds are resistant to oxidation and their rigid porous structure can prevent aggregation of nanoscale metal hydrides by limiting the movement and physical contact of individual particles during cycles. Various carbon scaffolds such as activated carbon [57,60,61], CMK-3 [17,53,54], polymer [20,42,85], carbon nanotube [57,86,87], graphene derivatives [19,55-59] have been reported where they commendably enhance the cycling sta-

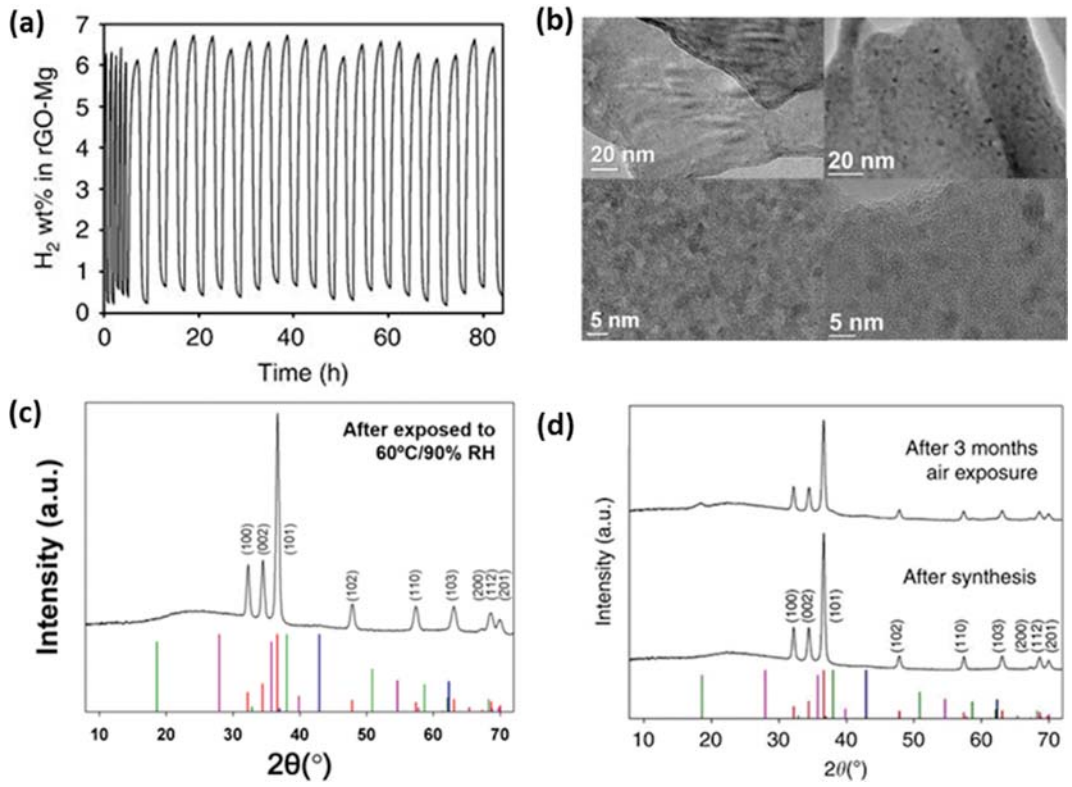

Fig. 7. (a) Hydrogen absorption/desorption cycling of rGO-Mg composite after exposure to air overnight. (b) TEM images of rGO-Mg after hydrogen cycling. XRD spectra of rGO-Mg (c) after exposure to 60 °C/90% RH in the environmental chamber and (d) after synthesis and after three months in air. Reprinted with permission from ref. [19], Copyright 2016 Springer Nature.

bility of metal hydrides by confinement. Among them, graphene derivatives exhibit outstanding performance with its unique physical and chemical properties. Cho et al. reported highly stable rGO-Mg laminates which have 3.26 nm-size of Mg crystal encapsulated in rGO [19]. The Mg crystal in this composite was stable for 25 cycles and no aggregation or performance degradation was observed (Fig. 7(a)). The encapsulated Mg crystals were well dispersed in rGO so that they did not come into contact with each other and maintained this structure even after the cycle (Fig. 7(b)). The other groups also reported Mg [58,59] and MgH_2 [55-57,88] nanocrystal which were similarly synthesized with graphene, and they exhibited an improvement in durability as well. Complex hydrides also take advantage of nanoconfinement with carbon scaffolds. During the desorption process, complex hydrides decompose as intermediates and the agglomeration of these intermediates significantly reduces reversibility. Carbon scaffold prevents the migration and agglomeration of these intermediates, thereby improving the repetitive storage property [42,49,76,89-94].

In addition to aggregation, oxidation of metal hydrides has also a vital effect in hydrogen storage performance. In general, dehydrogenated metal hydrides easily react with oxygen and moisture in air. For MgH_2, Mg even can be oxidized in an open vacuum condition during desorption step to form MgO or $Mg(OH)_2$. Metal oxide and hydroxide like MgO and $Mg(OH)_2$ are not able to react with hydrogen and significantly impede hydrogen sorption compared to bulk metal state. Moreover, those oxidized metals are hardly restored to zero-valent metal state or hydride form; therefore, oxidation of metal also causes enormous loss in storage capacity. Hence, protecting the surface from oxidation is important for permanent use of metal hydrides without deterioration. The confinement in carbon scaffolds effectively prevents the oxidation of metal hydride. The Mg crystals in rGO showed an excellent oxidation stability in high humid atmosphere at 60 °C and even after several months under ambient condition [19] (Fig. 7(c), (d)). This is due to the molecular sieving effect of graphene which only allows the penetration of hydrogen, not oxygen or water molecule. Also, the role of thin surface oxide layers as oxidation barrier for Mg nanocrystal within graphene was elucidated by Wan et al. [58] and Zhang et al. [59]. This thin oxide layer of Mg is formed through limited oxidation in graphene layers, effectively suppressing further oxidation of Mg crystals without deteriorating hydrogen storage performance.

3. Catalytic Effects of Scaffolds on Hydrogen Storage Performance

Carbon scaffolds not only stabilize metal hydrides but also enhance the sorption thermodynamic and kinetics. This improvement partially comes from the nanoscaling effect as particles are confined to the nano-sized pores, and it also largely attributed to the interaction effect between scaffolds and metal hydrides at the interface. The nano-sizing effects have already been elucidated in the preceding section (section 4.1), thereby focusing on the catalytic effects of carbon scaffold in this section.

A catalytic effect through carbon scaffolds is typically considered as an effect from carbon itself and an additionally functional-

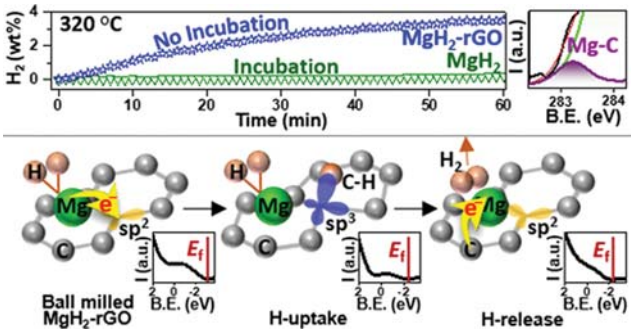

Fig. 8. Mg-C interaction induced enhanced hydrogen desorption performance of MgH_2-rGO nanocomposites in which Mg donates electron to sp^2 carbon in rGO during ball-milling and hydrogen absorption step, subsequently recovering it during desorption. Adapted with permission from ref. [96], Copyright 2018 American Chemical Society.

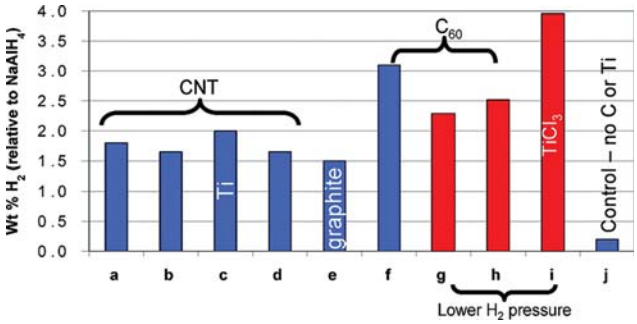

Fig. 9. Relative catalytic activity of carbon nanomaterials and $TiCl_3$ in $NaAlH_4$. Carbon materials with high curvature showed superior catalytic activity. Adapted with permission from ref. [90], Copyright 2009 American Chemical Society.

ized moiety such as transition metal or electron-rich hetero atom (N, P, etc.). A common mechanism is charge transfer at the interface of metal hydrides and catalyst. Jia et al. [95] reported a significantly reduced reaction enthalpy and entropy of MgH_2 confined within CMK-3. They claimed that the charge transfer between unsaturated carbon in CMK-3 and Mg caused Mg-H bond instability,j which allows easier release of hydrogen from Mg. A similar mechanism has been proposed for a composite of ball milling graphene and MgH_2. Shriniwasan et al. [96] synthesized MgH_2-rGO composite by ball-milling and showed that the Mg-C bond formed during the ball milling reaction greatly improved the desorption rate of MgH_2 (Fig. 8). Through a ball-milling and hydrogenation step, Mg donated electron to π^* orbital of rGO, and this caused the formation of C-H bond along with the weakened π band. The newly formed sp^3 structure of rGO was recovered during desorption cycle with hydrogen release from carbon. With the dissociation of hydrogen, electrons occupy the π and π^* orbital, and the π^* electrons are back-donated from carbon to Mg, weakening the Mg-H bond. Besides, a myriad of studies have reported the enhanced hydrogen storage performance of Mg with carbon scaffolds, which includes not only the above-mentioned CMK-3 [17, 61] and graphene [19,55-59], but also graphite [62], porous carbon and carbon nanotube [62,86] etc. [17,60,62].

However, the effects of carbon have not been fully understood in all metal and complex hydrides. The interaction between carbon and $NaAlH_4$ is considered not as effective as the case of Mg. Stavila et al. [49] and Gao et al. [92] reported nanoconfined $NaAlH_4$ in MOF and in nanoporous carbon separately. Both composites showed an improvement in kinetics and thermodynamics as well as reversibility; however, the authors claimed that the enhancement was based on the confinement effect which restricts the movement of Al during desorption cycles and nano-sizing effect of $NaAlH_4$, without any catalytic effect from the scaffolds. Especially, Gao's group argued that the comparable activation energy of $NaAlH_4$ in a similar particle size regardless of supporting materials was strong evidence that indicates the reduction of size is a dominant factor of enhancement by nanoconfinement, not an interaction with scaffold. Berseth et al. [90] also reported that only electronegative carbon matrices with high curvature such as fullerenes have catalytic effects on the desorption kinetics of $NaAlH_4$. The catalytic performance of various carbon materials with $NaAlH_4$ is shown in Fig. 9 [90].

The catalytic effects of carbon scaffolds can be enhanced by additional doping agents. These doped substances, such transition metals or hetero-atoms, improve hydrogen storage performance by accelerating hydrogen diffusion and/or dissociation. In the case of transition metals, the extended d-orbital mediates the electron transfer between Mg and hydrogen, acting as a catalyst [97]. Especially, nickel reacts with Mg and forms Mg_2Ni alloy which significantly facilitates the hydrogen diffusion [97,98]. In this regard, many studies have modified carbon scaffolds with transition metal such as Ti [49,88,93,94,99,100] and Ni [21,54,69,72,101-103]. Doping of some electron-rich elements (N, P) has also been reported to contribute to improved hydrogen storage performance [53,54].

CONCLUDING REMARKS AND PERSPECTIVES

In this review, we have introduced various scaffold materials for nanoconfinement of metal hydrides and discussed their effects on hydrogen storage performance, particularly focusing on carbon scaffolds. Carbon materials play multiple roles in improving hydrogen sorption properties of metal hydrides-not only producing nanoscaled metal hydride particles, but also providing a structural stability, simultaneously offering catalytic effects. These effects have been explained based on understanding of hydrogen sorption mechanism of metal hydrides, along with their kinetic and thermodynamic limits.

A remarkable development has been accomplished in hydrogen-based energy technologies including hydrogen storage, and currently we are witnessing hydrogen powered vehicles and domestic fuel cells. For hydrogen storage, material-based solid-state storage is the ultimate goal due to its high storage density and guaranteed safety. With a rational material design which utilizes various building blocks, such as carbon scaffolds, hydrogen storage performance based on metal hydrides has significantly improved; however, further advancement is required so that they can be used in practical application. For example, we have to enhance the infiltration/encapsulation efficiency of metal hydrides since incorporation of scaf-

fold materials inevitably causes dead mass, lowering hydrogen storage capacity. In addition, it is necessary to boost catalytic effects for alleviating operation temperature up to 85 °C. Furthermore, the modified hydrogen sorption mechanism in newly developed material systems should be underpinned in detail via reliable experimental and computational tools so that the related thermodynamic and kinetic properties can be elucidated to ensure the technological reproducibility. Although these tasks still remain to be resolved, we anticipate that further advancement of solid-stated hydrogen storage will eventually provide sustainable solutions to energy and climate challenges.

ACKNOWLEDGEMENTS

This work was supported by the International Energy Joint R&D Program of the Korea Institute of Energy Technology Evaluation and Planning (KETEP), granted financial resource from the Ministry of Trade, Industry & Energy, Republic of Korea (No. 20188520000570).

REFERENCES

1. K. Hyun, S. Kang and Y. Kwon, *Korean J. Chem. Eng.*, **36**(3), 500 (2019).
2. S. Kim, J. Song and H. Lim, *Korean J. Chem. Eng.*, **35**(7), 1509 (2018).
3. S. Dunn, *Int. J. Hydrogen Energy*, **27**(3), 235 (2002).
4. L. Schlapbach and A. Züttel, *Nature*, **414**(6861), 353 (2001).
5. J. Tollefson, *Nature*, **464**(7293), 1262 (2010).
6. M. Felderhoff, C. Weidenthaler, R. von Helmolt and U. Eberle, *Phys. Chem. Chem. Phys.*, **9**(21), 2643 (2007).
7. M. D. Allendorf, Z. Hulvey, T. Gennett, A. Ahmed, T. Autrey, J. Camp, E. S. Cho, H. Furukawa, M. Haranczyk, M. Head-Gordon, S. Jeong, A. Karkamkar, D.-J. Liu, J. R. Long, K. R. Meihaus, I. H. Nayyar, R. Nazarov, D. J. Siegel, V. Stavila, J. J. Urban, S. P. Veccham and B. C. Wood, *Energy Environ. Sci.*, **11**(10), 2784 (2018).
8. N. A. A. Rusman and M. Dahari, *Int. J. Hydrogen Energy*, **41**(28), 12108 (2016).
9. I. P. Jain, C. Lal and A. Jain, *Int. J. Hydrogen Energy*, **35**(10), 5133 (2010).
10. H. Shao, G. Xin, J. Zheng, X. Li and E. Akiba, *Nano Energy*, **1**(4), 590 (2012).
11. J. Yang and S. Hirano, *Adv. Mater.*, **21**(29), 3023 (2009).
12. T. Asefa, K. Koh and C. W. Yoon, *Adv. Energy Mater.*, **9**(30), 1901158 (2019).
13. S. Satyapal, J. Petrovic, C. Read, G. Thomas and G. Ordaz, *Catal. Today*, **120**(3), 246 (2007).
14. Q. Lai, Y. Sun, T. Wang, P. Modi, C. Cazorla, U. B. Demirci, J. R. Ares-Fernandez, F. Leardini and K.-F. Aguey-Zinsou, *Adv. Sustain. Syst.*, **3**(9), 1900043 (2019).
15. A. Schneemann, J. L. White, S. Kang, S. Jeong, L. F. Wan, E. S. Cho, T. W. Heo, D. Prendergast, J. J. Urban, B. C. Wood, M. D. Allendorf and V. Stavila, *Chem. Rev.*, **118**(22), 10775 (2018).
16. Y. Sun, C. Shen, Q. Lai, W. Liu, D.-W. Wang and K.-F. Aguey-Zinsou, *Energy Storage Mater.*, **10**, 168 (2018).
17. M. Konarova, A. Tanksale, J. N. Beltramini and G. Q. Lu, *Nano Energy*, **2**(1), 98 (2013).
18. W. Liu and K.-F. Aguey-Zinsou, *J. Mater. Chem. A*, **2**(25), 9718 (2014).
19. E. S. Cho, A. M. Ruminski, S. Aloni, Y.-S. Liu, J. Guo and J. J. Urban, *Nat. Commun.*, **7**(1), 10804 (2016).
20. K.-J. Jeon, H. R. Moon, A. M. Ruminski, B. Jiang, C. Kisielowski, R. Bardhan and J. J. Urban, *Nat. Mater.*, **10**(4), 286 (2011).
21. E. S. Cho, A. M. Ruminski, Y.-S. Liu, P. T. Shea, S. Kang, E. W. Zaia, J. Y. Park, Y.-D. Chuang, J. M. Yuk, X. Zhou, T. W. Heo, J. Guo, B. C. Wood and J. J. Urban, *Adv. Funct. Mater.*, **27**(47), 1704316 (2017).
22. V. Bérubé, G. Radtke, M. Dresselhaus and G. Chen, *Int. J. Energy Res.*, **31**(6-7), 637 (2007).
23. N. S. Norberg, T. S. Arthur, S. J. Fredrick and A. L. Prieto, *J. Am. Chem. Soc.*, **133**(28), 10679 (2011).
24. A. San-Martin and F. D. Manchester, *J. Phase Equilib.*, **8**(5), 431 (1987).
25. N. B. Arboleda Jr., H. Kasai, K. Nobuhara, W. A. Diño and H. Nakanishi, *J. Phys. Soc. Jpn.*, **73**(3), 745 (2004).
26. A. Züttel, *Mater. Today*, **6**(9), 24 (2003).
27. K.-F. Aguey-Zinsou and J.-R. Ares-Fernández, *Energy Environ. Sci.*, **3**(5), 526 (2010).
28. B. Sakintuna, F. Lamari-Darkrim and M. Hirscher, *Int. J. Hydrogen Energy*, **32**(9), 1121 (2007).
29. P. Heitjans and S. Indris, *J. Mater. Sci.*, **39**(16), 5091 (2004).
30. T. Hongo, K. Edalati, M. Arita, J. Matsuda, E. Akiba and Z. Horita, *Acta Mater.*, **92**, 46 (2015).
31. Y. Pang and Q. Li, *Int. J. Hydrogen Energy*, **41**(40), 18072 (2016).
32. M. H. Mintz and Y. Zeiri, *J. Alloys Compd.*, **216**(2), 159 (1995).
33. P. E. de Jongh and P. Adelhelm, *ChemSusChem*, **3**(12), 1332 (2010).
34. K.-F. Aguey-Zinsou and J.-R. Ares-Fernández, *Chem. Mater.*, **20**(2), 376 (2008).
35. S. B. Kalidindi and B. R. Jagirdar, *Inorg. Chem.*, **48**(10), 4524 (2009).
36. J. C. Crivello, B. Dam, R. V. Denys, M. Dornheim, D. M. Grant, J. Huot, T. R. Jensen, P. de Jongh, M. Latroche, C. Milanese, D. Milčius, G. S. Walker, C. J. Webb, C. Zlotea and V. A. Yartys, *Appl. Phys. A*, **122**, 97 (2016).
37. B. Paik, I. P. Jones, A. Walton, V. Mann, D. Book and I. R. Harris, *Philos. Mag. Lett.*, **90**(1), 1 (2010).
38. J. M. Sander, L. Ismer and C. G. Van de Walle, *Int. J. Hydrogen Energy*, **41**(13), 5688 (2016).
39. S. X. Tao, W. P. Kalisvaart, M. Danaie, D. Mitlin, P. H. L. Notten, R. A. van Santen and A. P. J. Jansen, *Int. J. Hydrogen Energy*, **36**(18), 11802 (2011).
40. L. Pasquini, M. Sacchi, M. Brighi, C. Boelsma, S. Bals, T. Perkisas and B. Dam, *Int. J. Hydrogen Energy*, **39**(5), 2115 (2011).
41. A. Baldi, M. Gonzalez-Silveira, V. Palmisano, B. Dam and R. Griessen, *Phys. Rev. Lett.*, **102**(22), 226102 (2009).
42. R. Gosalawit-Utke, S. Meethom, C. Pistidda, C. Milanese, D. Laipple, T. Saisopa, A. Marini, T. Klassen and M. Dornheim, *Int. J. Hydrogen Energy*, **39**(10), 5019 (2014).
43. S. S. Makridis, E. I. Gkanas, G. Panagakos, E. S. Kikkinides, A. K. Stubos, P. Wagener and S. Barcikowski, *Int. J. Hydrogen Energy*, **38**(26), 11530 (2013).
44. F. Peru, S. Garroni, R. Campesi, C. Milanese, A. Marini, E. Pellicer, M. D. Baró and G. Mulas, *J. Alloys Compd.*, **580**, S309 (2013).
45. A. F. Gross, J. J. Vajo, S. L. Van Atta and G. L. Olson, *J. Phys. Chem.*

C, **112**(14), 5651 (2008).
46. C. L. Carr, W. Jayawardana, H. Zou, J. L. White, F. El Gabaly, M. S. Conradi, V. Stavila, M. D. Allendorf and E. H. Majzoub, *Chem. Mater.*, **30**(9), 2930 (2018).
47. P. Ngene, P. Adelhelm, A. M. Beale, K. P. De Jong and P. E. De Jongh, *J. Phys. Chem. C*, **114**(13), 6163 (2010).
48. R. K. Bhakta, J. L. Herberg, B. Jacobs, A. Highley, R. Behrens, N. W. Ockwig, J. A. Greathouse and M. D. Allendorf, *J. Am. Chem. Soc.*, **131**(37), 13198 (2009).
49. V. Stavila, R. K. Bhakta, T. M. Alam, E. H. Majzoub and M. D. Allendorf, *ACS Nano*, **6**(11), 9807 (2012).
50. S. Chumphongphan, U. Filsø, M. Paskevicius, D. A. Sheppard, T. R. Jensen and C. E. Buckley, *Int. J. Hydrogen Energy*, **39**(21), 11103 (2014).
51. C. B. Minella, I. Lindemann, P. Nolis, A. Kießling, M. D. Baró, M. Klose, L. Giebeler, B. Rellinghaus, J. Eckert, L. Schultz and O. Gutfleisch, *Int. J. Hydrogen Energy*, **38**(21), 8829 (2013).
52. L. Li, X. Yao, C. Sun, A. Du, L. Cheng, Z. Zhu, C. Yu, J. Zou, S. C. Smith, P. Wang, H.-M. Cheng, R. L. Frost and G. Q. Lu, *Adv. Funct. Mater.*, **19**(2), 265 (2009).
53. D. He, Y. Wang, C. Wu, Q. Li, W. Ding and C. Sun, *Appl. Phys. Lett.*, **107**(24), 243907 (2015).
54. Y. Jia and X. Yao, *Int. J. Hydrogen Energy*, **42**(36), 22933 (2017).
55. G. Liu, Y. Wang, C. Xu, F. Qiu, C. An, L. Li, L. Jiao and H. Yuan, *Nanoscale*, **5**(3), 1074 (2013).
56. G. Xia, Y. Tan, X. Chen, D. Sun, Z. Guo, H. Liu, L. Ouyang, M. Zhu and X. Yu, *Adv. Mater.*, **27**(39), 5981 (2015).
57. Y. Huang, G. Xia, J. Chen, B. Zhang, Q. Li and X. Yu, *Prog. Nat. Sci.*, **27**(1), 81 (2017).
58. L. F. Wan, Y.-S. Liu, E. S. Cho, J. D. Forster, S. Jeong, H.-T. Wang, J. J. Urban, J. Guo and D. Prendergast, *Nano Lett.*, **17**(9), 5540 (2017).
59. J. Zhang, Y. Zhu, H. Lin, Y. Liu, Y. Zhang, S. Li, Z. Ma and L. Li, *Adv. Mater.*, **29**(24), 1700760 (2017)
60. T. K. Nielsen, K. Manickam, M. Hirscher, F. Besenbacher and T. R. Jensen, *ACS Nano*, **3**(11), 3521 (2009).
61. Z. Zhao-Karger, J. Hu, A. Roth, D. Wang, C. Kübel, W. Lohstroh and M. Fichtner, *Chem. Commun.*, **46**(44), 8353 (2010).
62. Q. Zhang, Y. Huang, T. Ma, K. Li, F. Ye, X. Wang, L. Jiao, H. Yuan and Y. Wang, *J. Alloys Compd.*, **825**, 153953 (2020).
63. C. Z. Wu, P. Wang, X. Yao, C. Liu, D. M. Chen, G. Q. Lu and H. M. Cheng, *J. Alloys Compd.*, **414**(1), 259 (2006).
64. Y. Liu, J. Zou, X. Zeng, X. Wu, H. Tian, W. Ding, J. Wang and A. Walter, *Int. J. Hydrogen Energy*, **38**(13), 5302 (2013).
65. R. Gosalawit-Utke, C. Milanese, P. Javadian, J. Jepsen, D. Laipple, F. Karmi, J. Puszkiel, T. R. Jensen, A. Marini, T. Klassen and M. Dornheim, *Int. J. Hydrogen Energy*, **38**(8), 3275 (2013).
66. M. Dieterich, C. Pohlmann, I. Bürger, M. Linder and L. Röntzsch, *Int. J. Hydrogen Energy*, **40**(46), 16375 (2015).
67. Y. Li, G. Zhou, F. Fang, X. Yu, Q. Zhang, L. Ouyang, M. Zhu and D. Sun, *Acta Mater.*, **59**(4), 1829 (2011).
68. L. F. Wan, E. S. Cho, T. Marangoni, P. Shea, S. Kang, C. Rogers, E. Zaia, R. R. Cloke, B. C. Wood, F. R. Fischer, J. J. Urban and D. Prendergast, *Chem. Mater.*, **31**(8), 2960 (2019).
69. J. Zhang, Y. Zhu, X. Zang, Q. Huan, W. Su, D. Zhu and L. Li, *J. Mater. Chem. A*, **4**(7), 2560 (2016).
70. S. Kim, H. Song and C. Kim, *Anal. Sci. Technol.*, **31**(1), 1 (2018).
71. H. Wang, S. F. Zhang, J. W. Liu, L. Z. Ouyang and M. Zhu, *Mater. Chem. Phys.*, **136**(1), 146 (2012).
72. G. Liu, Y. Wang, F. Qiu, L. Li, L. Jiao and H. Yuan, *J. Mater. Chem.*, **22**(42), 22542 (2012).
73. J. L. C. Rowsell and O. M. Yaghi, *J. Am. Chem. Soc.*, **128**(4), 1304 (2006).
74. X. Lin, I. Telepeni, A. J. Blake, A. Dailly, C. M. Brown, J. M. Simmons, M. Zoppi, G. S. Walker, K. M. Thomas, T. J. Mays, P. Hubberstey, N. R. Champness and M. Schröder, *J. Am. Chem. Soc.*, **131**(6), 2159 (2009).
75. D.-W. Lim, J. W. Yoon, K. Y. Ryu and M. P. Suh, *Angew. Chem. Int. Ed.*, **51**(39), 9814 (2012).
76. R. K. Bhakta, S. Maharrey, V. Stavila, A. Highley, T. Alam, E. Majzoub and M. Allendorf, *Phys. Chem. Chem. Phys.*, **14**(22), 8160 (2012).
77. A. S. Awad, M. Nakhl, M. Zakhour, S. F. Santos, F. L. Souza and J. L. Bobet, *J. Alloys Compd.*, **676**, 1 (2016).
78. S. S. Shinde, D. H. Kim, J. Y. Yu and J. H. Lee, *Nanoscale*, **9**(21), 7094 (2017).
79. V. Berube, G. Chen and M. S. Dresselhaus, *Int. J. Hydrogen Energy*, **33**(15), 4122 (2008).
80. S. Zhang, A. F. Gross, S. L. Van Atta, M. Lopez, P. Liu, C. C. Ahn, J. J. Vajo and C. M. Jensen, *Nanotechnology*, **20**(20), 204027 (2009).
81. A. Ampoumogli, T. Steriotis, P. Trikalitis, E. G. Bardaji, M. Fichtner, A. Stubos and G. Charalambopoulou, *Int. J. Hydrogen Energy*, **37**(21), 16631 (2012).
82. W. Li, C. Li, H. Ma and J. Chen, *J. Am. Chem. Soc.*, **129**(21), 6710 (2007).
83. C. Zhou, Z. Z. Fang and R. C. Bowman, *J. Phys. Chem. C*, **119**(39), 22261 (2015).
84. C. Zhou, Z. Z. Fang, R. C. Bowman, Y. Xia, J. Lu, X. Luo and Y. Ren, *J. Phys. Chem. C*, **119**(39), 22272 (2015).
85. A. M. Ruminski, R. Bardhan, A. Brand, S. Aloni and J. J. Urban, *Energy Environ. Sci.*, **6**(11), 3267 (2013).
86. J.-j. Liang and W. C. P. Kung, *J. Phys. Chem. B*, **109**(38), 17837 (2005).
87. J. Yuan, Y. Zhu, Y. Li, L. Zhang and L. Li, *Int. J. Hydrogen Energy*, **39**(19), 10184 (2014).
88. Y. Wang, L. Li, C. An, Y. Wang, C. Chen, L. Jiao and H. Yuan, *Nanoscale*, **6**(12), 6684 (2014).
89. C. P. Baldé, B. P. C. Hereijgers, J. H. Bitter and K. P. de Jong, *Angew. Chem. Int. Ed.*, **45**(21), 3501 (2006).
90. P. A. Berseth, A. G. Harter, R. Zidan, A. Blomqvist, C. M. Araújo, R. H. Scheicher, R. Ahuja and P. Jena, *Nano Lett.*, **9**(4), 1501 (2009).
91. R. D. Stephens, A. F. Gross, S. L. Van Atta, J. J. Vajo and F. E. Pinkerton, *Nanotechnology*, **20**(20), 204018 (2009).
92. J. Gao, P. Adelhelm, M. H. W. Verkuijlen, C. Rongeat, M. Herrich, P. J. M. van Bentum, O. Gutfleisch, A. P. M. Kentgens, K. P. de Jong and P. E. de Jongh, *J. Phys. Chem. C*, **114**(10), 4675 (2010).
93. T. K. Nielsen, M. Polanski, D. Zasada, P. Javadian, F. Besenbacher, J. Bystrzycki, J. Skibsted and T. R. Jensen, *ACS Nano*, **5**(5), 4056 (2011).
94. L. Zang, W. Sun, S. Liu, Y. Huang, H. Yuan, Z. Tao and Y. Wang, *ACS Appl. Mater. Interfaces*, **10**(23), 19598 (2018).
95. Y. Jia, C. Sun, L. Cheng, M. A. Wahab, J. Cui, J. Zou, M. Zhu and

X. Yao, *Phys. Chem. Chem. Phys.*, **15**(16), 5814 (2013).
96. S. Shriniwasan, T. Kar, M. Neergat and S. S. V. Tatiparti, *J. Phys. Chem. C*, **122**(39), 22389 (2018).
97. J. Cui, J. Liu, H. Wang, L. Ouyang, D. Sun, M. Zhu and X. Yao, *J. Mater. Chem. A*, **2**(25), 9645 (2014).
98. X. Huang, X. Xiao, X. Wang, C. Wang, X. Fan, Z. Tang, C. Wang, Q. Wang and L. Chen, *J. Phys. Chem. C*, **122**(49), 27973 (2018).
99. M. Lotoskyy, R. Denys, V. A. Yartys, J. Eriksen, J. Goh, S. N. Nyamsi, C. Sita and F. Cummings, *J. Mater. Chem. A*, **6**(23), 10740 (2018).
100. Y. Liu, H. Du, X. Zhang, Y. Yang, M. Gao and H. Pan, *Chem. Commun.*, **52**(4), 705 (2016).
101. Z. Lan, L. Zeng, G. Jiong, X. Huang, H. Liu, N. Hua and J. Guo, *Int. J. Hydrogen Energy*, **44**(45), 24849 (2019).
102. B. P. Tarasov, A. A. Arbuzov, S. A. Mozhzhuhin, A. A. Volodin, P. V. Fursikov, M. V. Lototskyy and V. A. Yartys, *Int. J. Hydrogen Energy*, **44**(55), 29212 (2019).
103. R. Xiong, G. Sang, G. Zhang, X. Yan, P. Li, Y. Yao, D. Luo, C. a. Chen and T. Tang, *Int. J. Hydrogen Energy*, **42**(9), 6088 (2017).

Eun Seon Cho is an Assistant Professor of Chemical and Biomolecular Engineering at Korea Advanced Institute of Science and Technology (KAIST). She obtained B.S. and M.S. degree in Materials Science and Engineering from Seoul National University and received her Ph.D. in Materials Science and Engineering in 2013 from Massachusetts Institute of Technology (MIT). She worked as a postdoctoral research fellow at Lawrence Berkeley National Lab from 2013 to 2017. Her works in the area of hydrogen storage focus on the development of nanostructured metal hydrides to enhance the hydrogen release and absorption properties. Her major research interests include the design and synthesis of functional hybrid nanomaterials with organic and inorganic building blocks for energy and environmental applications.